10-9-2008

# Determinants of Deforestation in Nepal's Central Development Region

Keshav Bhattarai

# Determinants of Deforestation in Nepal's Central Development Region

Keshav Bhattarai[1]

1. Dept. of Geography, University of Central Missouri, Warrensburg, MO 64093
(e-mail: bhattarai@ucmo.edu, Phone: 660-543-8805)

## Abstract

*The process of deforestation in the Central Development Region (CDR) of Nepal is diverse in space and time, with rapid deforestation still occurring in areas outside the national parks and wildlife reserves. This paper identifies the spatial driving forces (SDFs) of deforestation in CDR for 1975-2000 using satellite data of 1975 (MSS), 1990 (TM), and 2000 (ETM+) along with socio-demographic and socioeconomic variables. Radiometrically calibrated satellite images are individually classified into seven distinct classes and merged together to cover the entire CDR. Classification accuracies are also assessed. Areas of land use and cover within the areas of each Village Development Committees (VDCs) and municipalities are calculated from the classified images by overlaying vector files of 1,250 VDCs. A transition matrix is generated for 1975-1990 using classified images of 1975 and 1990 and then this product is used to further develop another transition matrix for 1990 - 2000 with the classified ETM+ 2000 images as the final stage. The VDC's vector layer of land use and cover areas is overlaid on the transition matrices to calculate deforestation areas by VDCs for 1975-1990 and 1990-2000. A digital elevation model (DEM) compiled from 35 ASTER scenes taken on different dates is used to examine areas at different elevation levels: 30-1,199 m, 1,200 – 2,399 m, 2,400- 4,999 m, and >5,000 m. Only the first three elevation levels are used in the analysis because area > 5,000 m is under permanent snow cover where human related forestry activities are almost negligible. Biophysical and socioeconomic information collected from various sources is then brought into a geographic information systems (GIS) platform for statistical analyses. Six linear regression models are estimated using SAS; in effect, two models for each elevation range representing 1975-1990 and 1990-2000 periods of change to identify SDF influences on deforestation. These regression analyses reveal that deforestation in the CDR is related to multiple factors, such as farming population, genders of various ages, migration, elevation, road, distance from road to forest, meandering and erosion of river, and most importantly the conversion of forestland into farmland.*

**Keywords:** Nepal, Forest, Remote Sensing, MSS, TM, ETM+, Village Development Committee, DEM

**Introduction:**

Most research on land use and land cover dynamics (LUCD) in the 1970s and 1980s focused on tropical regions of South American countries (Laney 2004; Nepstad, *et al*, 1999; Whitmore 1997). With close to half of the world's tropical forests now impacted by human settlement, LUCD research in less developed countries has increased considerably since then. This LUCD literature suggests that an integration of biophysical and socioeconomic information will help to identify proximate and causal spatial driving forces (SDFs) of deforestation in specific geographic contexts at local and regional-scales (Armenteras, *et al*, 2005; Aspinall, 2004; Chowdhury, 2006; Deininger and Minten, 2002; Ferreira, *et al*, 2006; Pfaff, *et al*, 2007). However, such literature often lacks the incorporation of national level policies and practices, and much of it has been characterized as 'aspatial'. Furthermore, it generally fails to embed socio-demographic information of the resident populations with biophysical data, such as elevation, aspects, slopes, rivers, distance from road to forest, and length and area of roads, so that interactional effects can be assessed.

To address some of these oversights, this paper integrates both 'aspatial' and spatial data including elevation, aspects, and slopes and socioeconomic information to identify the SDFs that influence LUCD in one severely impacted South Asian country, Nepal. It examines the heuristic effects of SDFs to reveal the spatial relationships between dominant drivers of LUCD, which otherwise would not have been unearthed by simply analyzing spatial data. We utilize three elevation levels of Nepal's Central Development Region (CDR) to represent their respective ecological zones to examine how SDFs influence deforestation at these three elevation levels or zones; namely

tropical and subtropical (30-1,199 m), temperate (1,200-2,399 m), sub-alpine and alpine (2,400-4,999 m) zones. We do not include areas >5,000 m because this is above the permanent snow line. We choose CDR and divide it into three elevation belts for several reasons: a) this region represents landscape ranging from 30 to 7,100 meters elevations covering tropical, subtropical, temperate, alpine sub-alpine and snow belts; b) during the 1975-2000 period, this CDR region experienced the most rapid land use and cover change in comparison to the other four (far western, mid-western, western, and eastern, Figure 1b) development regions of the country; c) its population density is relatively high (at 293 people/kilometer as compared to 164 national average) in Nepal; d) there are rapid social and demographic changes underway due to the location in the CDR of several urban administrative centers including the Kathmandu Valley, the capital city; and e) the first community forestry program that started in Nepal, especially at the >1,200 m elevation level, began in this region in 1978.

Bhattarai (2001) and Bhattarai and Conway (2008) have identified SDFs using aspatial (socioeconomic) and spatial (remote sensing) data for the Bara districts, one of the 19 districts of the CDR. Elsewhere, Chowdhury (2006), Ferreira *et. al.*(2006), Skole and Tucker (1993), Sader (1995), and Soares-Filho *et.al.* (2006) have studied the influences of SDFs on LUCD and their impacts on ecosystems. Nepal, Bohara, and Barrens (2007) used an econometric model to examine linkages between the strength and type of social networks in private forest conservation activities in rural Nepal. However, this later model did not use spatial variables.

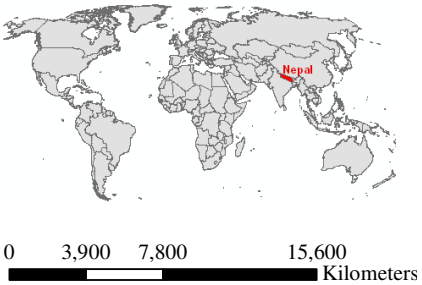


Fig.1a: The World showing Nepal

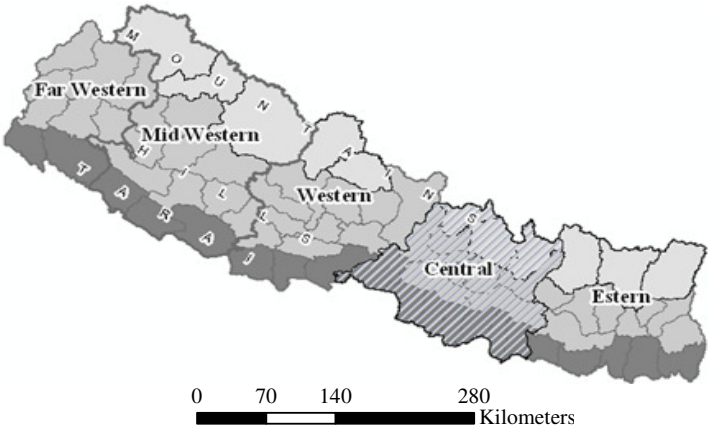


Fig. 1b: Nepal showing the Central Development Region

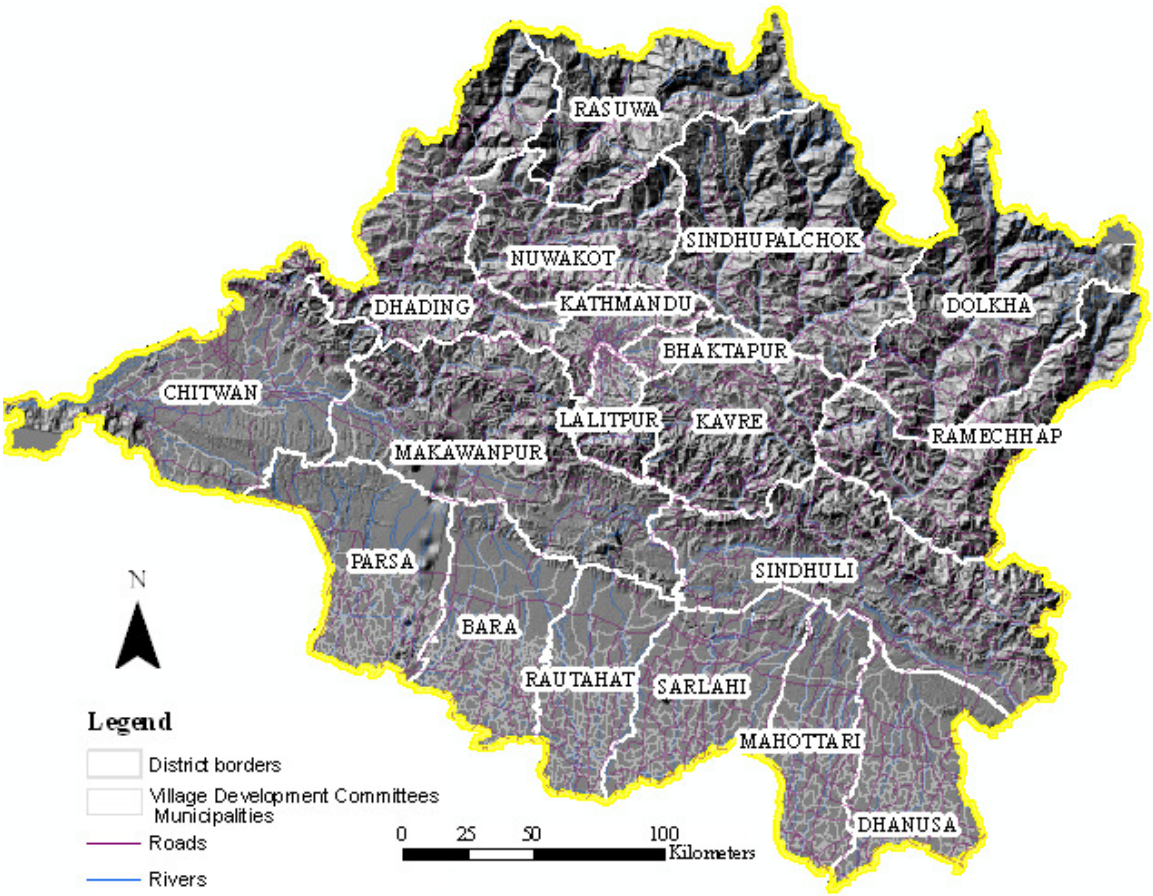


Fig. 1c: Topography of Central Development Region showing district boundaries, Village Development Committee/Municipality boundaries, roads, and rivers.

A large body of literature analyzes the causes of deforestation, but very rarely does it analyze the causes of deforestation at various elevation levels with respect to the

ecological variations they bring about. The major goals of this paper, therefore, are to determine the extent of deforestation at various elevation levels and to specifically test the following set of hypotheses concerning the expected influences of SDFs on deforestation's patterns in the CDR of Nepal:

a. the extent of anthropogenic (human) influences on deforestation and afforestation, assessed from satellite imagery, will vary among tropical and subtropical, temperate and sub-alpine and alpine belts, in large part because of the differences in natural resource bases and human settlement dynamics in these ecological zones.
b. the activities of in-migrants accelerate the rate of deforestation;
c. Community forestry approaches are effective means to conserve and manage forests and thus to preserve greenery in higher elevation belts.
d. The higher the elevation the less is the population pressure on forest, but deforestation occurs due to biophysical factors.

We estimate the areas of deforestation from transition matrices and integrate this information into 1,192 Village Development Committees (VDCs), 21 municipalities, two sub-metropolitan and one metropolitan urban areas of 19 districts of the CDR; all of which are distributed among three ecological zones at 30-1,199 m, 1,200-2,399 m, and 2,400-4,999 m elevations. However, in the analysis, we exclude five urban areas of the Kathmandu Valley, namely Bhaktapur, Kathmandu, Kirtipur, Lalitpur, and Madhyapur Thimi, and one sub-metropolitan—Birgunj--located in the southern part. We also exclude two national parks and one wildlife reserve from the model estimations. The reasons for excluding urban areas are due to the nonexistent of forest in urban areas, and strict

protection of national parks and reserve by the Nepal Army. Even after the exclusion of these areas, it leaves us with 1,245 variables (records) in the model. Actually, there are fewer than 1,215 VDCs and urban areas in this region, but the 1,245 records are due to the divisions of some VDCs into more than one polygon through national, political gerrymandering processes. Some politicians did the gerrymandering seeking favorable election results. In fact, one VDC or municipality can extend to various elevation ranges; therefore, when these 1,245 records were categorized into different elevation ranges, we arrive at 1,085 records for 30-1,199 m, 609 records for 1,200-2,399 m and 221 records for 2,400-4,999 m elevations. We did not use areas >5,000 m in the analysis because not much human-related forestry activity has occurred at this elevation range. After this introductory background, the rest of the paper presents a theoretical framework, study area, data, the models and their outcomes, discussions, conclusion, and finally references.

**2. Theoretical framework:**

Deforestation results from the expansion of the non-forested area as human beings use forest resources for various purposes. The analysis of the causes and consequences of deforestation involves complex interrelations because it results from the effects of different driving forces; some of these forces might be accelerating or decelerating. Human settlements and roads have been identified as accelerating factors for deforestation (Pfaff 1999; Rudel 1989). In less accessible remote areas, deforestation occurs due to natural causes at the beginning, but later as the technology advances, deforestation progresses rapidly (Dull, 2007). Slowly, anthropogenic-led forces advance deforestation towards less accessible sites including higher elevations and steep terrains

as many factors synergistically act together. However, some government policies, such as community forestry, people participatory approaches to forestry development and conservation, often decelerate deforestation processes in certain geographic locations where forest products are less commoditized (Bhattarai *et al*., 2002).

Ideally, any identification of deforestation processes would need sophisticated methods because not only is this process influenced by anthropogenic forces, but also by topographical conditions such as elevation, slope and aspect. Populations living in specific geographic locations and utilizing their own specific cultural traditions at different elevations and in different ecological regimes exert pressures on forest resources that should be expected to differ. Therefore, variables such as elevation, slopes, aspects, population age-cohort, migratory status, the locational effects on accessibility by rivers and roads are essential to include in an explanatory model. A cursory examination of the effects of topography on vegetation is possible by integrating information obtained from a relief map with satellite images, but more detail analyses require an integration of digital elevation information with classified satellite images. Socioeconomic conditions also influence deforestation processes, therefore, it is essential to include socioeconomic information specific to different geographic locations.

Since the 1990s, a number of studies have attempted to explicate the dynamics of land use and cover in local and regional-scale analyses by combining remote sensing data with spatially referenced biophysical and socioeconomic information (Armenteras *et al*., 2005; Aspinall, 2004; Chowdhury, 2006; Ferreira *et al*. 2006; Pfaff *et. al*. 2007). Not only have these studies identified the locations and proximate causes of land use and cover dynamics, but also they have identified the fundamental driving forces and tested various hypotheses concerning these forces.

Rapid progress in remote sensing technology has led to the advancement of various theories, which integrate both aspatial and spatial explanations. Such theories were mostly oriented economically (Chomitz and Thomas 2003; Chowdhury 2006; Nelson *et al.* 2001; Walker 2004). Land allocation theories postulated by Von Thünen, and Ricardo were used to predict land use dynamics as a function of market integration, environmental factors, and agricultural land use (Chowdhury, 2006). Geoghegan *et al.* (2001); Munroe *et al.*(2004); Pfaff (1999); and Rindfuss and Walsh (2003) used spatial modeling techniques to identify spatial and temporal driving forces of land use dynamics, while Ruttan and Hayami, (1984) and Laney (2004) used agricultural intensification theories to understand the influence of SDF on land use dynamics. SDF models have also been used to examine the impacts of land access and use policies, such as infrastructure development and government incentives to people (Cropper *et al.*, 1999; Walker and Solecki, 2004). While the above approaches use both empirical and spatial models, Irwin and Geoghegan (2001) made important distinctions between these two models. They argued that the empirical model could be of theoretical significance, while the later model could explain human behaviors at specific geographic locations. Additionally, the spatial model uses methodological diversity beyond satellite image classification and even includes regional environmental history. Vasquez-Leon and Liverman (2004) emphasized political ecological frameworks to explain land use dynamics. Bhattarai and Conway (2008) took farm forestry approaches to assess land use dynamics, while Turner *et al.* (1996) based their work on their own ecological framework for such analyses. Rindfuss *et al.* (2007) used complex interactions between the demographic and environmental conditions to explain land use dynamics using both aspatial and spatial data. Nelson and Hellerstein (1995) analyzed the effects of roads on deforestation and Dull (2007) observed a direct relationship between deforestation and road

construction. He observed accelerated deforestation after the construction of roads in the low flat areas first, and then in the interior areas. He concluded that large tracts of forest will be limited only in the higher and least accessible areas. Rudel (1989) observed that population pressure was one of the common correlates of deforestation. Like roads, Dull (2007) also observed that deforestation occurred close to rivers due to their high flow velocities that resulted in the under-cutting of proximate banks and nearby lands leading to landslides. Deforestation also occurred in association with river meandering after the deposition of debris on the river beds caused flooding, new channel-formation, and forest destruction.

**3. Study area:**

The central development region (CDR) of Nepal (Figure 1c) sustains 37% of the country's population within 19% of its geographic area and experiences a heightened central role in the nation's overall development because of the location of the country's primary urbanized core and administrative center, the Kathmandu Valley, within its boundaries. Such has been the extent of urbanization and urban sprawl at the expense of rural and non-urban cover in the Valley, however, that this region is omitted from our analysis, so as not the unduly influence or bias the region-wide results. The Central Development Region (Figure 1b) extends into three main physiographic regions—mountains (5%), hills (73%), and Tarai (22%)--and has experienced the highest deforestation rate in the country. Examining and specifying each national physiographical region's analytical sub-unit mix, the mountain region is divided into 51 VDCs and one municipality, the hills into 501 VDCs, 11 municipalities, one sub-metropolitan, and one

metropolitan areas, while the Tarai is divided into 585 Village Development Committees (VDCs), 10 municipalities, and one sub-metropolitan administrative area.

**4. DATA:**

This research uses biophysical (land use and land cover, roads, rivers, slopes, aspects, and elevations), socio-demographic and socioeconomic data (population, age group, income, land holding, occupations, migrant status) at the Village Development Committees (VDCs) level, which is the smallest administrative division of Nepal. Because the integration of such a plethora of socioeconomic and biophysical data poses problems due to their different units of measurement and differences in spatial data projection systems, uniform measurement units are used in our statistical models. For example, all areas are estimated in square meters, lengths are also in meters, and absolute population numbers represent the demographic pressure at the VDC level.

In term of spatial alignment of data, since most of the maps of Nepal are projected to the modified UTM Zone 44.5 N (average of 45 and 44 zones), the images and vector files available to us require projection and re-projection into modified UTM, Zone 44.5 N using specific correction measurements for better alignments and data integrations. These specific parameters include Spheroid-Everest, Quadrant NE, XSHIFT (-) 400000, YSHIFT 0, PARAMETERS—Longitude $84^0$ 00' 00" E and Latitude $26^0$ 15' 00" N. Such projections help us integrate spatial information available from the Survey Department of the Government of Nepal with remotely sensed data.

**4.1. Satellite Data:**

This research uses the Multispectral Scanner (MSS) imagery of 1975, Thematic Mapper (TM) imagery of 1990 and Enhanced Thematic Mapper (ETM+) of 2000 (Figure 2). Landsat data archives cover most of the Earth's terrestrial surface between 81° N and 81° S latitudes and have a relatively long temporal extent—1972 to present day. All these satellites return to the same location after a certain time, providing successive images of most regions except those plagued by interminable periods of cloud cover – which includes some densely forested regions in the tropics – where intermittent temporal coverage is the unfortunate reality. The Landsat 2 (MSS) sensor used to return to the same sky space and repeatedly captures scenes of an area every 18 days from 900 kilometers (km) height, while Landsat 5 (TM) and Landsat 7 (ETM+) do so every 16 days from 705 km and cover a swath width of approximately 185 × 185 km.

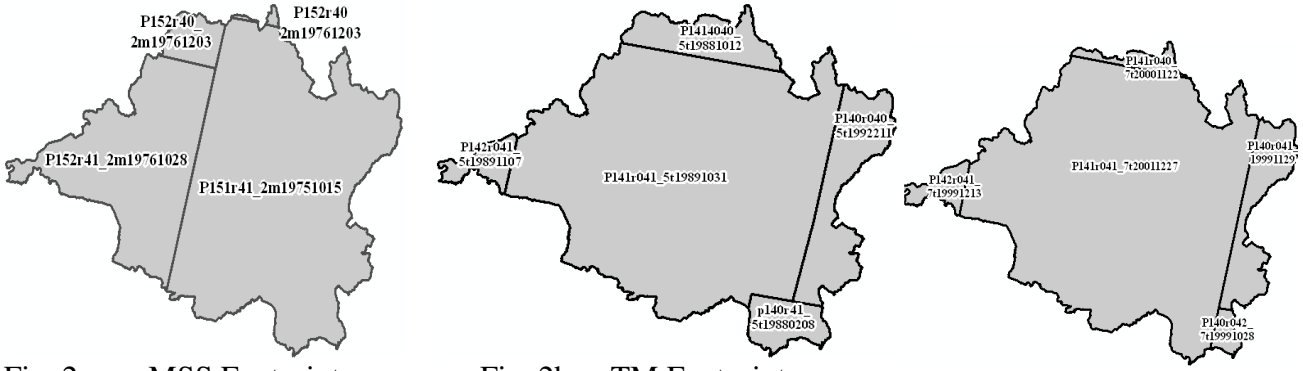


Fig. 2a MSS Footprints Fig. 2b TM Footprints Fig. 2c ETM Footprint

Figure 2: Images (footprints) used in the study

Our objective was to access usable satellite images at three-time points, 1975, 1990, and 2000 to compare the rates of deforestation for the periods, 1975-1990 and 1990-2000. It would have been best if all the images of the base years we acquired had been taken on the same dates and months for 1975, 1990, and 2000, but this was not possible due to excessive cloud cover

some of the times the satellites passed. However, we were able to get data of MSS for 1975 and 1976, TM for 1989, 1990, 1991, and 1992, and ETM+ for 1999, 2000, and 2001. Though these images were taken at different dates, imagery data for 1975, 1990, and 2000 covered the most part of the CDR and therefore we are able to capture the interesting patterns of the base years. Given the particular vegetation phonology in Nepal, most of the vegetation contains minimum amounts of leaf moisture during the months of October, November, December, January, and February, so that images taken during these months clearly measure and monitor the land use and cover scenes. Thus, we are confident that our image data capture the major phenological characteristics and land use and cover trends of 1975, 1990, and 2000 of the region.

The ortho-rectified TM 1990 and ETM+ 2000 images were downloaded from the University of Maryland website and MSS 1975 and 1976 images were acquired from the EROS Data Center, while some MSS images of 1976 were also downloaded from http://glovis.usgs.gov/. The MSS images were geo-referenced against the ETM+ images using the WGS 84 datum and spheroid with a root mean square (RMS) error of less than 0.5 following the image-to-image geo-referencing system. Visual verification of geo-referencing accuracy is accomplishing by overlaying various image bands in the ERDAS Imagine 9.1. After the geo-referencing, all images are radiometrically calibrated using ATCOR in Erdas Imagine 9.1

**4.2. Radiometric Calibration:**

Satellite images can have anomalies due to the presence of noise, inconsistent detector responses, sensor malfunctioning, atmospheric interference, and differences in illumination and viewing geometry due to topographic variations. In order to remove these anomalies and to normalize images, it is essential to calibrate them radiometrically. Radiometric calibration also helps to correct intra-and-inter-instrumental differences,

instrumental drift, variations in earth-sun distances ($d_{sun}$), and different solar zenith angles ($\theta_{sun}$). In our research, sensors' standardization is essential because of the uses of different sensors. These different sensors in Landsat respond linearly to incoming radiance from the earth-atmospheric system, which are described by slope and intercept values for each band. These slope and intercept values are then corrected by using the engineering names, gains and biases given in the header files of images (Lillesand, Kiefer, and Chipman, 2008). Header files provide information such as the amount of light, instrument's gain--slope, bias--intercept, bandpass values, $d_{sun}$, and $\theta_{sun}$ for each specific date of a band for each image.

The calibration makes the narrower near infrared band (4) of TM [and ETM+] images comparable with the combined bands of the MSS that detects the plant vigor (Lillesand *et al*. 2008). In the calibration, visible and near infrared bands of MSS (1, 2, 3, and 4) and visible, near and mid infrared Landsat TM and ETM+ bands (1, 2, 3, 4, 5, and 7) are converted into digital numbers (DNs) to a quantitative physical surface reflectance values. For each band, slope and intercept values are used to adjust DN values by multiplicative and additive terms. All the DN values are converted into radiance to make them comparable at the satellite apparent at-sensor radiance for each band.

In theory, image calibration corrects any linear differences due to instrumentation and noises present in the atmosphere (Lillesand *et. al*., 2008); however, a comparison of results of a radiometrically calibrated classified image *vs*. un-calibrated images shows very little or almost no impact on the final land use and cover results. This is probably because, with most classifiers, the algorithm is designed to assess relative differences among pixel values. However, remote sensing literature suggests the calibration of

Landsat images by using standard light sources with known radiometric intensities to calibrate spectral wavelength displacement. In this process, radiance that reaches a sensor, $L_s$ is expressed by:

$$L_S = K.DN + L_{\min}\,(Wm^{-2}Sr^{-1})$$
$$and, K = \frac{L_{\max} - L_{\min}}{DN_{range}} \qquad \text{---------- (i)}$$

where,

DN = digital number (image gray level value), $L_{max}$ and $L_{min}$ = maximum and minimum radiance (measurement of the brightest and darkest objects in the dataset), $DN_{range}$= the difference between the largest and smallest digital number in the dataset, $L_S$ = watt per meter-squared per steradian.

Once calibration is done for each individual image using the standard radiometric techniques, all images are separately classified following a hybrid method of unsupervised and supervised classifications.

**4.3. Classifications:**

All images are classified individually because the images of different dates could have specific spectral properties, different from other images. Theoretically, calibration could bring all the images to the atmospheric radiance values. Merging all the radiometrically calibrated images should not produce any anomalous results after classification; however, errors are observed when all the images were merged before classification. Therefore, all images are classified separately according to a guided classification scheme using Erdas Imagine 9.1, and we use combined unsupervised and supervised classification techniques. Initially, an unsupervised Iterative Self-

Organizing Data Analysis Technique (ISODATA) routine was run on Landsat bands 1, 2, 3 and 4 of MSS and 1–5 and 7 of TM and ETM+ to cluster individual images into 25 classes. These classes are visually analyzed using flicker to visualize and assign specific class names. Spectral profile curves are used to examine the objects' reflection by electromagnetic radiations. Pixels that correspond to clouds, land surfaces under cloud shadows, and shadows caused by the terrain (about 5-7% of the image area) are then removed from the images. The remaining portions of the image areas are then clustered into 20 classes by a second ISODATA routine. Clusters are labeled to specific land-cover classes, and signatures of the labeled clusters of each image are used as the basis for a supervised maximum likelihood classification of the individual images. Class names are assigned to various land use and cover classes. The roads and rivers identification on the classified images are reconfirmed by overlaying the vector layers available from the Department of Survey, Nepal; if abnormalities were noticed, images were reclassified. After the proper identification of roads and rivers, they are extracted from the images as separate raster files through recoding, if raster == roads or rivers, then 1, otherwise, 0. We calculated the areas covered by the rivers and roads from the images of 1975, 1990, and 2000. After the separation of these road and river into layers, these classes are merged with the bareland because the bareland and road and river showed overlapping values (1550 - 1680 ≈ 1700) in the transformed divergence index. Eventually, we end up having eight classes through recoding; these include mature forest, secondary growth, degraded forestland, farmland, barren, water, cloud, and no data.

Land use and cover classes are verified following *a priori* knowledge of one of the authors who worked in this area for 13 years (1983-1995). Some areas not confirmed in 1975 image from *a priori* knowledge were cross-checked using the aerial photos and topographic

maps of 1976-1978, and 1988-1989 aerial pictures, and topographic maps of 1992 are used to verify the land use and cover classes in the 1990 images. Cross validation of ETM+ 2000 classified images is done using the IKONOS (1m x 1m) images taken in 2003. These cross-validations are only conducted on selected complex mosaics of land use and land cover areas where the boundaries between forest and non-forest areas are not clear. The guiding assumption for this is that forest seen on IKONOS 2003 is forest in 2000.

Accuracy assessments are done for each individual image using the maximum likelihood method. In accuracy assessment, parameters such as 1024 search count and 150 numbers of points are chosen in the "Add Random Points" dialog to examine the accuracy of land use classes representing all three elevation an ecological zones of the CDR. In all the classification accuracy assessments, contingency matrices are generated to examine overall accuracy; Kappa statistics, the procedural- and user- accuracies following standard classification processes as suggested by Lillesand *et al.* (2008). Kappa values quantify how much better a particular classification is when compared to a random classification, making it possible to calculate a confidence interval for comparing two or more classifications. Procedural accuracy is generated to measure the percentage of pixels of a given land cover type that are correctly classified. User accuracy is generated to measure the commission errors useful for examining whether or not a pixel classified into a given class actually represents that class on the ground. We use a subjective scale in accuracy assessment and found Kappa values of greater than 80 percent for all the images, for which Monserud and Leemans (1992), categorize as yielding 'excellent' results.

After checking the accuracy, all individual images are subset to the actual classified areas and mosaics made to the base images of 1975, 1990, and 2000 to cover the entire region. These mosaic images are re-sampled to 60 m x 60 m to bring them to

the same resolution; for example, all MSS images are upgraded to 60 m x 60 m from 80 m x 80 m, while the TM and ETM+ images are degraded to 60 m x 60 m from 28.5 m x 28.5 m. The decision to resample the images into 60 m x 60 m is made after no significant information errors are found between the re-sampled and original images. After these re-samplings, the land use and land cover classes of three elevation levels belonging to 1,915 VDCs and municipalities are computed for three years—1975, 1990, and 2000 (Figures 3 a-c).

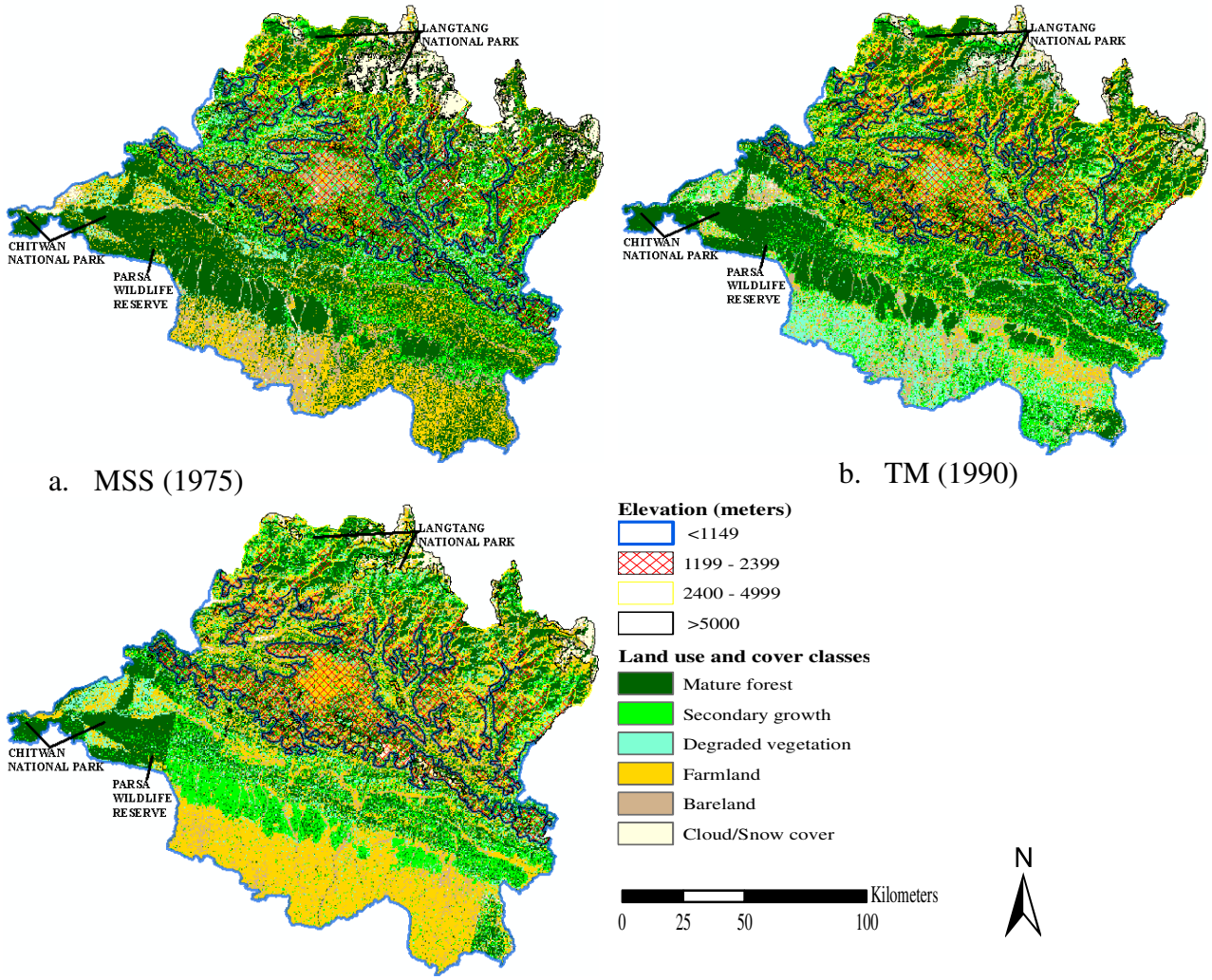


a. MSS (1975)

b. TM (1990)

c. ETM (2000)

Figure 3: Land use and land cover classes for 1975-2000 by elevation classes

**4.3. Digital Elevation Model (DEM)**:

The elevation data is collected from the Advanced Spaceborne Thermal Emission and Reflection Radiometer (ASTER) sensor. The ASTER sensor was launched on December 16, 1999 in collaboration with Japan (JPL) and NASA and acquires scenes for a specific location every 16 days; with each scene covering approximately 60 km x 60 km swath width (Verma, 2002).

Starting in early summer of 2006, the Land Processes Distributed Active Archive Center (LP DAAC) has implemented new production software for efficiently creating quality DEMs with an automated stereo-correlation method, but without any ground control points (GCPs). The Land Processes Distributed Active Archive Center's (LPDAAC) website suggests that the DEM utilizes the ephemeris and altitude data derived from both the ASTER instrument and the Terra spacecraft platform. The new ASTER DEM is a single-band product with 30-meters horizontal postings that is geodetically referenced to the UTM coordinate system, and referenced to the Earth's geoid using the EGM 96 geopotential model. These ASTER DEMs are produced automatically with no manual editing. According to the USGS and NASA, the accuracy of the new LP DAAC-produced DEMs are more accurate than 25 meters root mean square errors for three dimensions (RMSE xyz). This 25 meters RMS error is good enough for this scale of analysis.

Altogether 24 DEM scenes are needed from the ASTER sensor to cover the CDR (Figure 4). The need for many overlapping scenes is due to the presence of cloud on images of various scenes. A portion of the cloud-free DEM scene is extracted from one scene covering a certain location and another cloud free scene is then used to cover other overlapping areas of the same scene's swath. Such situations required us to take many scenes to capture the whole CDR. Yet,

we did not find cloud free DEMs for two locations. For one location we interpolated surface to cover the uncovered area while for another location, we patch the blank area from Shuttle Radar Topography Mission (SRTM).

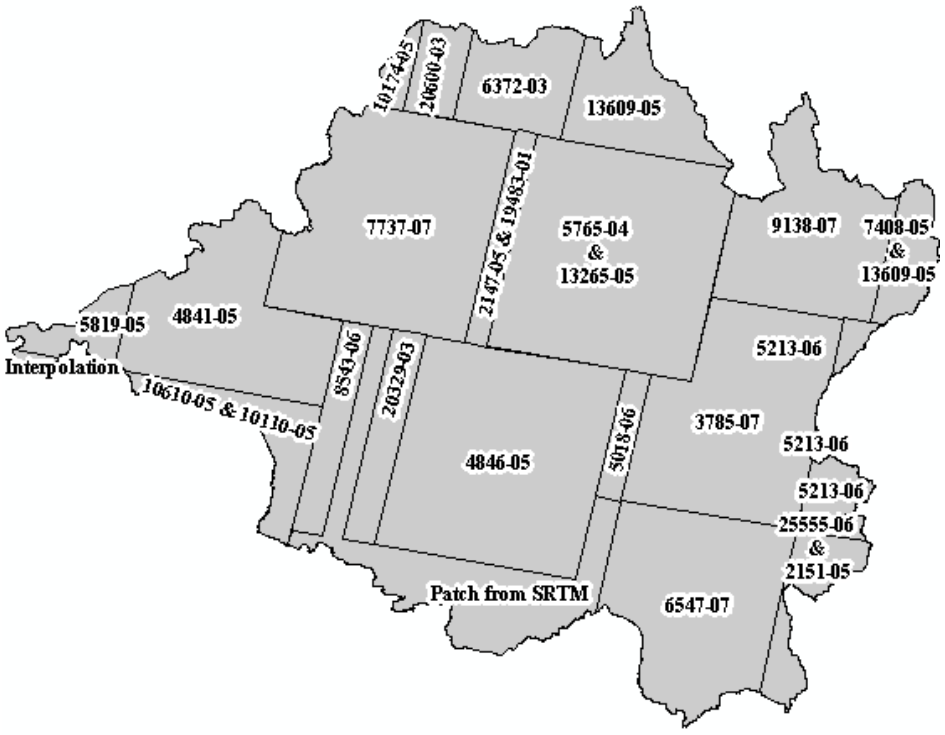


Figure 4: Foot prints of Digital Elevation Data from ASTER; in the figure, the identification number 7737-07 refers to the granule number (7737) and the year (07) when image was taken.

The DEM is re-sampled to 60 m x 60 m to match the resolution of the re-sampled classified satellite images and is used to calculate the areas of the four elevation classes. These are categorized into three operational levels and one redundant level, respectively: tropical and subtropical belts (30-1,199 m), temperate belts (1,200-2,399 m), sub-alpine and alpine belts (2,400-4,999 m) and above the snow line (> 5,000 m). To maintain the integrity of these elevation divisions as appropriate representatives of ecological zonal variation, quite a number of VDCs in the CDR are found in more than one elevation level. As a result, the original set of

1,245 VDC unit records are sub-divided into 1,915 records (Figure 5). We divide the total CDR region into three elevation belts because of the following reasons:

1. Stainton (1972) classified the area below <1,000 m as tropical and between 1001-2000 m as subtropical. Although Stainton (1972) classified the mixed broad-leaved forests extending from 1001- 2,000 m elevation into subtropical belt, we restrict our subtropical region to elevations up to 1,199 m because this elevation includes the southern foothills of Churia range including the Siwalik Hills and valleys and some of the dense riverine forests in the mid hills with high sub-tropical climatic conditions, where most of the forest areas were under the control of the government until 2000s. Within this elevation range, the mean winter daytime temperatures are between 22 and 27°C, whilst summer temperatures exceed 37°C. The biogeochemical cycle is very rapid where substantial plantations and natural forest of *Dalbergia sissoo*, *Eucalyptus spp*., *Tectona grandis* (Teak), *Shorea robusta* (Sal), and *Acacia catechu* (Khair), Terminalia spp. (Saj), *Anogeissus latifolia* (Aghrak), and *Bombax ceiba* (Simal) are growing.
2. We categorized the belt within 1,200-2,399 m as temperate, and it includes moist north- and west- facing slopes of the Siwalik and Mid-Hills in the CDR. This area is dominated by *Pinus roxburghii* (Chir Pine), *Alnus nitida*, *Castanopsis tribuloides*, *Castanopsis hystrix*, *Lithocarpus pachyphylla*, *Quercus spp,* and *Quercus semecarpefolia*. The average temperature of this belt being within the range of $12^0$-$16^0$ C plant growth is less vigorous than in the tropical and sub-tropical belts. Communities in this belt manage most of these forests.
3. We categorized the area within the 2,400-4,999 m elevation as sub-alpine and alpine. This belt contains mixed broad-leaved forest in the moister north- and west-facing slopes.

Acer, *Rhododendron spp*, *Aesculus*, *Pinus wallichiana*, *Cedrus deodara*, *Picea smithiana*, *Juniperus indica, Abies pindrow, Abies spectabilis*, *Betula utilis*, *Rhododendron spp*, and *Juglans spp* are the predominate species of this belt. Many forest areas are handed over to local communities for management.

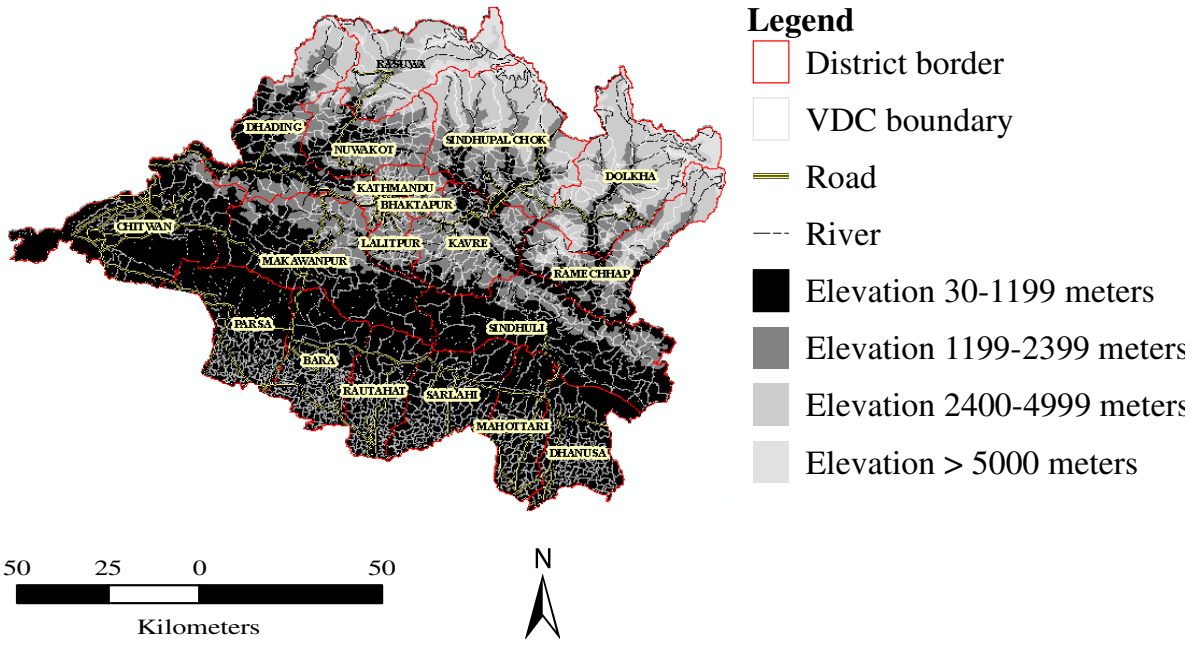


Figure 5: Central Development Region showing elevation (meters) with roads, rivers, and borders of VDC/Municipalities and Districts.

### 4.4. Roads and rivers layers:

Lengths of roads and rivers are calculated for 30-1,199 m, 1,200-2,399 m, 2,400 – 4,999 m elevation belts using VDCs' vector layers. These vector layers are overlaid on the 1975, 1990, and 2000 images. For the years 1975 and 1990, all roads are grouped into one class each (road1975 and road1990) for two reasons: first, except for the highways, other roads are not clearly identifiable on the classified satellite images; and second, the attribute table of the vector road layer, available from the Department of Survey of Nepal Government, does not provide

road classifications. For 2000, roads are classified into two classes--highways and 'others'. All the blacktopped and graveled roads are classified under highways, while all dirt roads are grouped under 'others'. The lengths and areas of roads and rivers for each three elevation levels are calculated by using the conditional functions in Spatial Analyst in ArcMap {CON([road or river grid] AND ([Elevation Class] = = conditional statement), conditional statement).

**4.5. Land use and cover dynamics (1975-2000):**

Land use and land cover classes are derived for 1975, 1990, and 2000 for 30-1,199 m, 1,200-2,399 m, and 2,400 – 4,999 m elevation levels. In this integration process, only five classes—mature forest, secondary growth, degraded vegetation, farmland, and bareland—are used for 1975, 1990, and 2000 (Figure 6). The classes under water, cloud and snow cover are ignored since they do not hold any significance in land use and cover dynamics. Though water bodies are important, the area covered by water is only a small fraction of the total area, mainly due to the depletion of surface water into debris on the riverbeds during the dry seasons when the images were sensed. The classified images of 1975, 1990, and 2000 revealed land use and land cover scenarios for three time points, however, these images do not display location specific changes in land use and cover between 1975-1990 and 1990 and 2000. Therefore, in order to get the location specific LUCD information, we generated two transition matrices for 1975-1990 and 1990-2000.

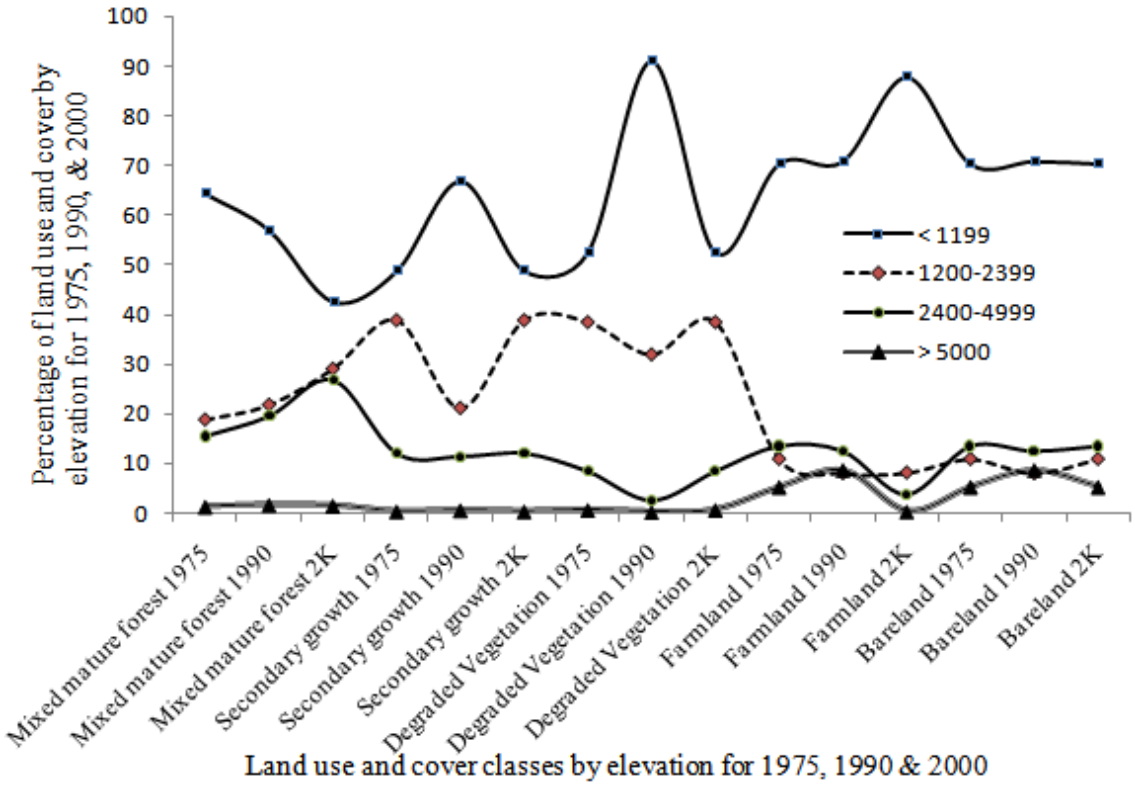


Figure 6: Trends of land use and land cover classes (1975-2000) by elevation

### 4.6. Transition matrices:

Two transition matrices are generated for 1975-1990 and 1990-2000 to examine the location specific effects of spatial driving forces on deforestation using the classified images. Matrix A (1975-1990) is developed using classified images of MSS 1975 and TM 1990, and Matrix B is developed by crossing matrix A with the classified ETM+ 2000. Using both matrices A and B, we examine the trends of deforestation and afforestation for 1975-1990 and 1990-2000 (Equation ii) at specific geographic locations (Figures 7).

$$Transition(T_{ij}) = \frac{n_{ij}}{\sum_{j=1}^{n} n_{ij}} \quad \text{.....(ii)}$$

Where, $T_{ij}$ is the transition between 1975 -1990 and 1990-2000, $n_{ij}$ is the number of transitions i ==> j occurred between 1975-1990 and 1990-2000. This shows the number of pixels that undergo changes from one period to another.

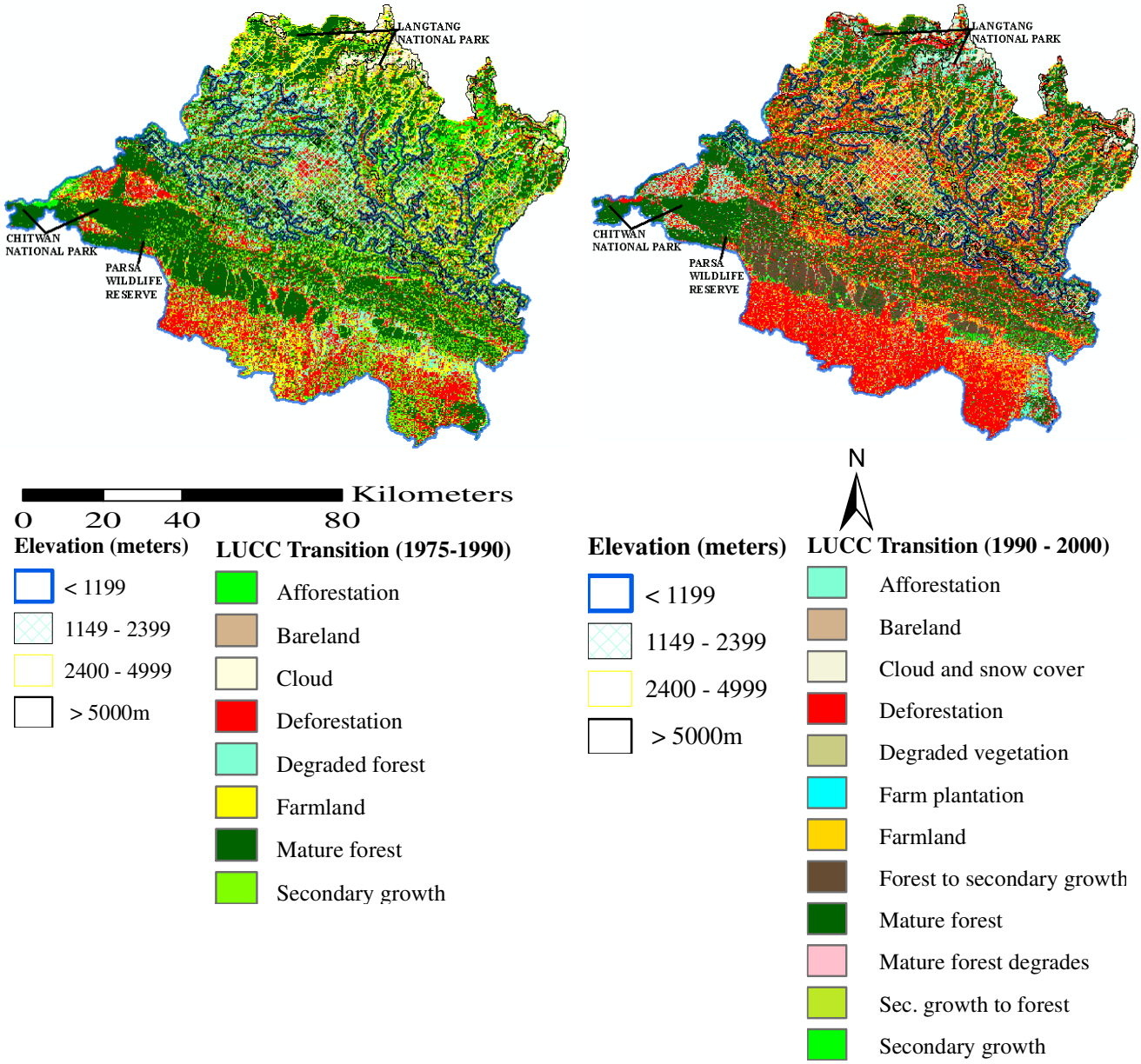


Figure 7: Transition matrices 1975-1990 and 1990-2000 by elevation

After generating the land use and land cover matrices A and B (Figure 7), deforestation layers are exported into ArcMap as grid files; these grid files are vectorized as polygon. These vector files are then clipped into three different elevation levels. Their areas are recalculated in

ArcMap and each polygon is converted into a centroid with the areas for each polygon attached to the centroids' attribute table for each VDC and municipality. The data of afforestation and deforestation for each 1,915 VDCs and municipalities are generated by overlay procedures. These data of afforestation, deforestation, and elevation are joined with the vector layers of VDCs and municipalities belonging to three elevation levels in ArcMap using the table-join procedures.

**4.7. Socioeconomic information:**

Socio-demographic and socioeconomic information incorporated into this model are as follows: population involved in agriculture, average land holdings by households, household population living on farm, numbers of poultry, and livestock, population by age-cohorts, economic activities, education and income levels, and migratory status. This information is obtained from the Central Bureau of Statistics of Nepal. All the sociodemographic and socioeconomic information were taken for the decennial census years because of the unavailability of the data for mid-decade (1975). For 2000, we gathered sociodemographic and socioeconomic information from the report jointly prepared by the Central Bureau of Statistics and National Planning Commission Secretariat, Nepal, and United Nations Population Fund (UNFPA). All these socioeconomic data are individually gridded using the inverse distance weighted function in Spatial Analyst in ArcGIS 9.2 using a power of two in order to generate data for 30-1,199 m, 1,200-2,399 m, 2,400 – 4,999 m elevation belts (Figures 8).

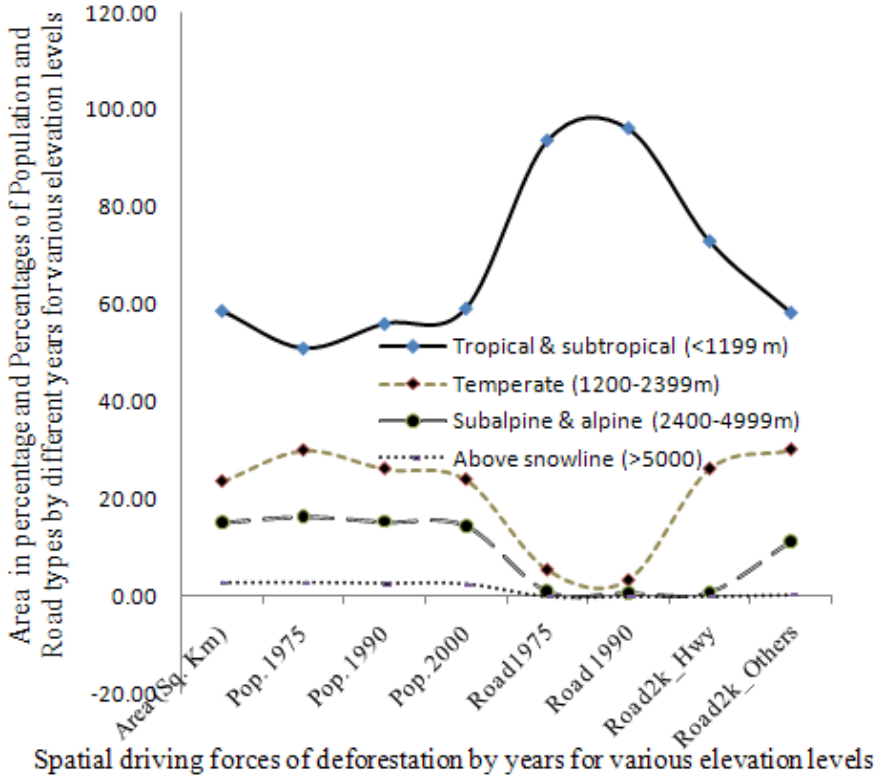


Figure 8: Relationships among area, population, and roads by elevation levels

Our modular approach to integrate different data is given in Figure 10 and models' outputs are presented in Tables 1.1-1.3. Using SAS 9.1, we generate six models: a) Model I'a' (1975-1990) and Model I'b' (1990-2000) for 30-1,199 m; b) Model II'a' (1975-1990) and Model II'b' (1990-2000) for 1,200-2,399 m; c) Model III'a' (1975-1990) and Model II'b' (1990-2000) for 2,400-4,999 m.

**4.8. Dependent variable:**

The dependent variable "deforestation" for the 1975 -1990 and 1990-2000 periods is derived from the transition matrices obtained from the classified satellite images for 30-1,199 m; 1,200 -2,399 m; 2,400 – 4,999 m elevation belts. Various reasons guided us for the selections of 1975-1990 and 1990-2000 for the three elevation classes (Figure 9).

1. Since 1978, His Majesty's Government of Nepal, now the Government of Nepal, started a community forestry program in the hills and mountains (approximately, >1,200 meters elevation) to conserve and promote forests through peoples' participatory approaches. Since then, the management responsibilities of many forest areas of the hills and mountains were transferred to the local communities in the names of Panchayat and Panchayat protected forests during the Panchayat regime (1960-1990), now the community forests and these community forests are less disturbed even during the time of several political upheavals (Gilmour and Fisher, 1991; Varughese, 2000).
2. There was a referendum in 1980 to choose between the partyless Panchayat System (1960-1990) and multiparty system. During this period, many Panchayat supporters were granted impunity to commercialize logging and to claim densely forested lands in the lower elevations in the south, hoping that the partyless Panchayat system will draw maximum public support, and also the people of hill origin could implant nationality feelings among the people of the Tarai region.
3. There was a pro-democracy revolution in 1989-1990 that changed the 230 years (1769-1990) of direct rule of king into a constitutional monarchy, with the establishment of Westminster bicameral parliamentary system of governance. During the pro-democracy movement, many areas were deforested, in large part because of the dysfunctional lack of governmental control the unrest brought about.
4. The period 1990-2000 is chosen because during this time many social and political problems were exacerbated due to the People's War operated by the

Communist Party (Maoist) that started in 1996 with the intention of overthrowing the constitutional monarchy. From 1996 to 2000, over 8,000 people were killed in the cross fires between the Maoist rebels and government forces, and many government institutions became even more dysfunctional than in previous eras.

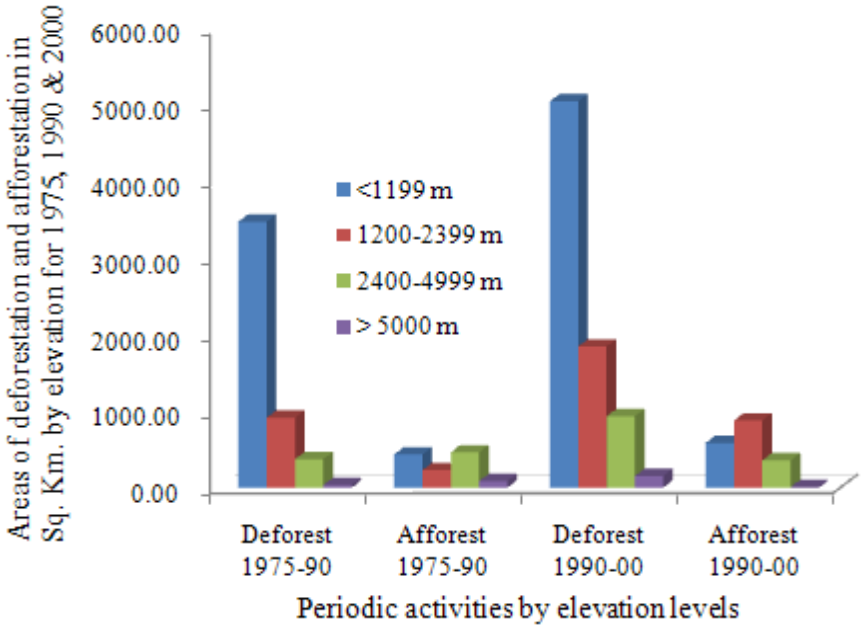


Figure 9: Deforestation and afforestation by elevation levels for 1975-1990 & 1990-2000

Spatial and aspatial data derived for the 1975-1990 and 1990-2000 are integrated into a GIS platform to examine the effects of spatial driving forces on the land use dynamics.

**5. The Model:**

After the integration, data are analyzed utilizing Statistical Analysis Software (SAS) to identify the determinants of deforestation. We choose Village Development Committees (500-20,000 people) and municipalities (>20,000) as our unit of analyses. Out of 1,250 VDCs, records

in the data, we utilize only 1,245 records belonging to 19 administrative districts of which seven belong to Tarai, eleven to hills, and one to mountain region (Figure 1). Again, these 1,245 administrative records are subdivided into 1,915 records as these VDCs and municipalities are divided into 30-1,199 m, 1,200-2,399 m, 2,400 – 4,999 m elevation levels. In each elevation level, we consider road accessibility and hydrological influences as space-variant and yet time dependent variables to examine the transitional probabilities for land use and cover changes. We develop the general model in four steps (Figure 10).

A. *Remotely sensed imaged are analyzed to map the spatial extent of forest losses for 1975, 1990 and 2000;*
B. *Transition matrices A and B are developed from these classified images;*
C. *The spatial information generated from remotely sensed images are brought into a GIS platform, and these data are integrated with sociodemographic and socioeconomic information;*
D. *Statistical analyses are performed to examine the relationships between the deforestation as dependent variable and other independent variables*

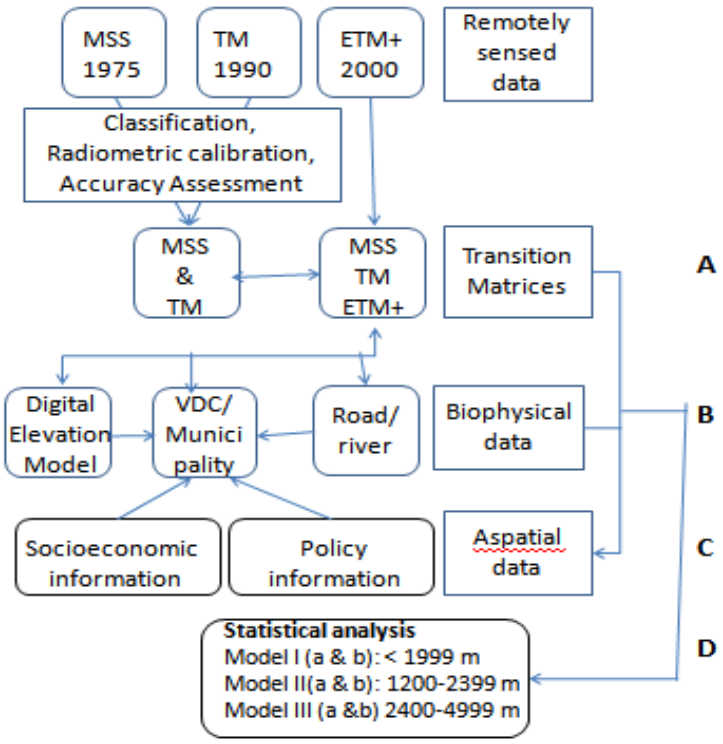


Figure 10: The Model

The goals of these steps are to develop, fit, and interpret stochastic models to clarify spatial processes that can explain the patterns of deforestation or more specifically the land use dynamics at various elevation levels. This is a rather challenging undertaking because of the intertwined effects of biophysical, sociodemographic, socioeconomic, and government policies. Even from several cross-national studies, scholars have applied Mills methods of negotiation (Rindfuss *et al*. 2007), because factors affecting deforestation vary across culture contexts and geographic locations. Nonetheless, the growing body of literature agrees that land use and land cover dynamics are inherently of a spatial nature. Therefore, it is worthwhile having many explanatory variables of deforestation as potential determinants. Granger (1998) lists at least 28 different variables, directly or indirectly linked to deforestation or land-use change in a forested

landscape, while Kaimowitz and Anglesen (1998) list 140 different causal variables that are believed to explain deforestation.

Several models have been used to examine the complexities of spatial driving forces (SDFs) on deforestation. Kaimowitz and Angelsen (1998), Pfaff (1999), Mertens and Lambin (2000), Napstad *et al*. (1999), and Geist and Lambin (2002) provide a summary of various types of tropical deforestation models. However, these models do not explicitly incorporate pre-modeling Remote Sensing-GIS procedures to reproduce the spatial patterns of changes in land cover and land use and deforestation and afforestation We do, by developing six linear regression models to estimate deforestation during the 1975-1990 and 1990-2000 periods for tropical and subtropical (30-1,199 m), temperate (1,200-2,399 m), and sub-alpine and alpine belts (2,400-4,999 m). We select individual variables by examining their roles in the deforestation processes using Chi-square ($\chi^2$) tests with the dependent variable--deforestation. We utilize only those variables in the model that show significant associations with deforestation in the Chi-square ($\chi^2$) test at specific elevation ranges (Tables 1.1-1.3).

**Table 1.3 goes here**

Regression Model Ia (tropical and subtropical belts) for 1975-1990 is presented in the following equation:

$$Y = \beta_0 + \sum_{i=1}^{11} \beta_i x_i \text{ ----------(iii)}$$

and the prediction $\hat{Y}$ is given by

$$\hat{Y} = \hat{\beta}_0 + \sum_{i=1}^{11} \hat{\beta}_i x_i$$

Where, $\hat{\beta}_0 = 730452$ , $\hat{\beta}_1 = 1350.85$ , $\hat{\beta}_2 = -11418$ , $\hat{\beta}_3 = -463.87$ , $\hat{\beta}_4 = 3185.98$ , $\hat{\beta}_5 = -16393$ , $\hat{\beta}_6 = 15343$ , $\hat{\beta}_7 = 8610.85$ , $\hat{\beta}_8 = -0.0822$ , $\hat{\beta}_9 = 0.36865$ , $\hat{\beta}_{10} = -260.47$ , $\hat{\beta}_{11} = 0.041$

Regression Model Ib (tropical and subtropical belts) for 1990-2000 is presented in the following equation:

$$Y = \beta_0 + \sum_{i=1}^{11} \beta_i x_i \text{ ----------(iv)}$$

and the prediction $\hat{Y}$ is given by

$$\hat{Y} = \hat{\beta}_0 + \sum_{i=1}^{11} \hat{\beta}_i x_i$$

Where, $\hat{\beta}_0 = 87051$ , $\hat{\beta}_1 = 170.89$ , $\hat{\beta}_2 = 2.48$ , $\hat{\beta}_3 = 176.05$ , $\hat{\beta}_4 = 613.76$ , $\hat{\beta}_5 = -651.24$ , $\hat{\beta}_6 = -535.30$ , $\hat{\beta}_7 = -1747.61$ , $\hat{\beta}_8 = -0.2525$ , $\hat{\beta}_9 = 0.95225$ , $\hat{\beta}_{10} = 1.9438$ , $\hat{\beta}_{11} = -0.00315$

## Table 1.2 goes here

Regression Model IIa (temperate belt) for 1975-1990 is presented in the following equation:

$$Y = \beta_0 + \beta_1 x_1 + \beta_2 x_2 + \beta_3 x_3 \text{ ----------(v)}$$

and the prediction $\hat{Y}$ is given by

$$\hat{Y} = -132277 + 11404\, x_1 + 0.12728 x_2 + 0.4068 x_3$$

Regression Model IIb (temperate belt) for 1990-2000 is presented in the following equation:

$$Y = \beta_0 + \beta_1 x_1 + \beta_2 x_2 + \beta_3 x_3 + \beta_4 x_4 + \beta_5 x_5 \text{ ----------(vi)}$$

and the prediction $\hat{Y}$ is given by

$$\hat{Y} = -25395 + 2926.51 x_1 - 28.24083 x_2 + 1.759 x_3 - 0.19256 x_4 + 0.89755 x_5$$

## Table 1.3 goes here

Regression Model IIIa (sub-alpine and alpine belts) for 1975-1990 is presented in the following equation:

$$Y = \beta_0 + \beta_1 x_1 + \beta_2 x_2 \text{ ----------(vii)}$$

and the prediction $\hat{Y}$ is given by

$$\hat{Y} = 2193779 - 0.60003x_1 + 0.13556x_2$$

Regression Model IIIb (sub-alpine and alpine belts) for 1990-2000 is presented in the following equation:

$$Y = \beta_0 + \beta_1 x_1 + \beta_2 x_2 \text{ ----------} (viii)$$

and the prediction $\hat{Y}$ is given by

$$\hat{Y} = 503472 + 0.63672x_1 + 0.74875x_2$$

In support of previous research that has established rivers, roads and their distances to forest areas as prime determinants of deforestation, our Chi-square ($\chi^2$) tests also reveal similar results.

**5.1 Tropical and sub-tropical sub-regions (30-1,199 m):**

Models' Ia & Ib for 1975-1990 reveal the significance of various driving forces, such as, immigrants (people migrating from the hill and mountain regions), population involved in transportation, male (20-29 years) and female (30-34 years) gendered, age cohorts, the conversion of forests into farmlands, and highways. The relationships between these independent variables and deforestation explain the ground reality. During the 1975-1990 period, the government of Nepal resettled people from the mountain and hill regions to the Tarai region to ease local pressures that had built in those long-populated areas and to settle the Tarai's tropical and subtropical forested frontier. The East-west Highway (Figure 5) was constructed during that period to help the nation's commercial sector with many people involved in trade, transportation, and the timber trade within Nepal and across India; with the latter being for the construction of railway sleepers there. The Timber Corporation of Nepal and Tarai Resettlement programs were

deeply involved in commercial logging and in the conversion of forestlands into farmlands at these lower elevations. At the same time, several commercial plantations were completed in afforestation projects supported by the World Bank, Asian Development Bank, and the European Union. Due to the concentrated development of roads and other infrastructure in this region, its nearness to the Indian markets, and increasing values of forest products in accessible areas, several forces can be seen acting synergistically to the hasten the deforestation in this belt (Equation iii). Though almost all the governmental forest offices lack logistic support for the protection and management of forests, driven by the need for revenue collection the government managed most of the forest areas with exploitation as its primary goal. Only a few forest areas were given to communities to manage. As a result, many forests were lost or degraded due to the concept that 'everyone's land is no body's land': the classic 'tragedy of the commons' that Hardin theorized in 1968. To this day, very few forests are transferred to local communities in this Tarai belt, when compared to the temperate, subalpine and alpine belts (Figure 11).

**5.2 Temperate Region (1,200-2,399 m):**

After the enactment of community forestry law in 1978, many forest areas were handed over to local communities for their management. Our model outcomes reveal that only a few SDFs are synergistically causing deforestation in this belt in 1975-1990 as compared to the tropical and sub-tropical belts during this same earlier period (Table 1.2, Equation iv). As further development took place in this temperate elevation belt during 1990-2000, roads have stronger influences on forests, local communities utilize the forest

to support their subsistence farming, and many forest areas have been converted into farmlands. Deforestation patches seen on the image for the 1975-1990 in this temperate belt could also be due to the after-effects of government policies of the Forest Nationalization Act 1957, which brought about the nationalization of any forest areas still present on private lands. Many private owners might have cleared forests from their lands to avoid this 'privatization' of their property. This indirect effect of the 1957 Act might also be the reason for the permanent conversion of forest into bare or farmlands and the possible edge effects of such clear-cutting on the nearby forests. Since government oversight and management has always been largely ineffective in many of Nepal's inaccessible areas, the Forest Nationalization Act 1957 appears to have had lasting effects for decades (Bajarcharya, 1983; Bhattarai *et al*., 2002; Gilmour and Fisher, 1991; Sen, Rao, and Saxena, 1997).

**5.3 Sub-alpine and alpine belts (2,400-4,900 m):**

Many local communities are actively involved in the management of community forests. Models' III a & IIIb outputs suggest that only a very few factors such as river erosion and farming activities are the determining factors of deforestation, in either the 1975-1990 period or the 1990-2000 period (Table 1.3, Equation viii).

**5.4 Hypothesis testing:**

Based on the model outputs (Tables 1.1-1.3), we test the following hypothesis.

*Hypothesis I: The extent of human disturbance, assessed from satellite imagery, will vary among tropical and subtropical, temperate and sub-alpine and alpine belts.*

A comparison of our research findings with the previous work by Muller-Boker (1999), who concluded that the main causes of deforestation in the lower belt were due to human settlements, reveals differences in the human disturbances in the higher and lower elevations. A review of literature reveals that in the early 1950s and 1960s, the lower belt of Nepal was considered unsafe for human settlements due to malarial problems. However, with the elimination of malaria in the late 1950s and early 1960s in the Tarai, road infrastructure was developed, encouraging the conversion of forests into farmlands. Previous research by two of the authors (Bhattarai, 2001; Bhattarai *et al*., 2002; Bhattarai and Conway, 2008; Conway, Bhattarai, and Shrestha, 2002) supported the conclusion that since the 1950s, infrastructure development, agricultural intensification, and government policies to convert forest into farmlands have been the primary causes of deforestation in certain parts of southern Nepal; notably in Bara and Bardiya . Flat areas adjacent to rivers become the preferred lands for new settlements and forests located in such areas often are the first ones to be converted into agricultural farmland. Image analyses reveal patterns of settlements and agricultural expansion along the flat areas of the region following road networks first and then expansion to the north along the foothills of Siwalik along the banks of river.

Over the last three-decades, the population of the Tarai lower belt has increased from 41 to 49% (Figure 8) due to constant in-migration from the north (Shrestha *et. al*., 1999). Figures 7 and 9 support our hypothesis that there are differences in the spatial extent of deforestation between tropical and subtropical and temperature belts with higher rates of deforestation being experienced in the south rather than the north. Our analysis of LUCD trends (Figures 8 and 11) and infrastructure development and population growth patterns across the whole CDR (Figure 8) emerge as similar to previous findings in the Bara district (Bhattarai *et. al.* 2002) that

deforestation accelerates after the development of infrastructure and population growth because forest products become a scarce commodity. The 1975 image analysis reveals forest area-clearance in the Siwaliks ranges (1000 m), but in 1990 and 2000 images deforestation is seen in the southern areas after the construction of roads.

With the development of roads from 1975-2000 at the lowest elevations < 1,199 meters, factors such as, immigrants ($p = <.0001$), population involved in transportation ($p = <.0107$), male population between the age cohort of 20-29 years ($p = <.0001$), female population between 30-34 years ($p = <.0001$), farmland ($p = <.0001$), population on farm, livestock, and poultry ($p = <.0001$), and highway 1975 ($p = <.0003$) all appear to contribute to deforestation in these tropical and sub-tropical zones. Though farmland increases and forest decreases might be expected to be correlated, the Durbin-Watson D = 1.782 and 1st Order autocorrelation = 0.099 tests do not reveal the two have a multi-collinear relationship. These findings match the earlier findings, where Bhattarai (2001) used a multinomial logistic regression model and found strong relationships between migrants' activities and deforestation in this region. However, for elevation 1,200 – 2,399 m, only a few factors, such as population depending upon livestock, poultry ($p = <.0001$), farmland ($p = <.0025$), and distance from road to forest ($p = <.0001$) have explained the deforestation without much multi-collinearity between dependent and independent variables (Table 1.2). Further north, in the zone between the elevations of 2,400-4,999 m, even fewer variables, such as erosion due to river ($p = 0.0225$) and farmland ($p = <.0001$) are significant. These significant values suggest that there are differences in the lower and higher elevations in LUCD.

*Hypothesis II: The activities of migrants accelerate the rate of deforestation;*

Model I (a & b, Table 1.1) suggest that the activities of migrants are clearly associated with deforestation in the lower hills, mainly because of the lack of other job opportunities and also because of the high cost of forest products within Nepal and across the Indian border in nearby local bazaars. Between 1975 and 2000, the population of the Tarai increased from 41% to 49% mainly due to the in-migration of people from the hills and mountains (> 1,200 m) regions and deforestation rate also increased from 1.6 – 2%.

*Hypothesis III: The community forestry approaches are effective means to conserve and manage forests and thus to preserve greenery in higher elevation belts.*

Figures 3, 6, 8, and 9 clearly reveal that there are more deforestation in the lower elevation than in the higher elevations. A review of the government records reveals that only a few community forests were handed over to local communities in the zones at lower elevations as compared to those at higher elevations (Figure 11). Community forests have survived even during severe political upheavals, while forests under the control of government suffer from the 'tragedy of the commons'.

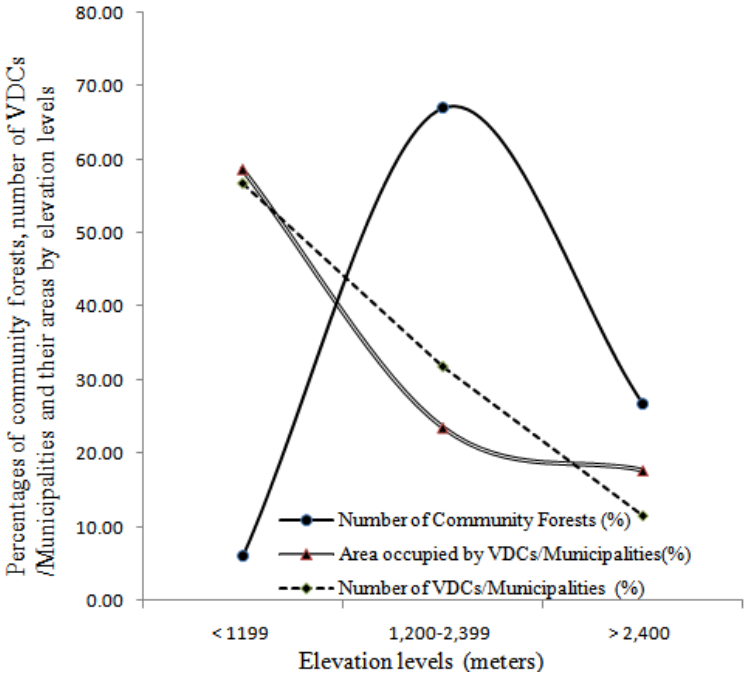


Figure 11: Number of community forests (%), areas occupied by VDCs/Municipalities (%)

*Hypothesis IV: The higher the elevation, the lower is the population pressure on the forest, but the loss of forest is due to river actions and over dependence of people on forests.*

Figure 8 reveals that the higher elevation has the fewest people, but the working age population is engaged in forest product collection, which often leads to widespread losses of forests. Similar to Quincey *et al*. (2006) and Tiwari's (2000) findings, we also observe losses of forest in these mountian zones due to fierce river action at such higher elevations (Table 1.3). Semwal *et al*. (2007) related the economic implications of river erosion and forest losses to the economic under-development of this mountainous part of the country. Ives and Messerli (1987) observed similar situations from their study of the middle hills of Nepal. The over-dependence of people on forests and river actions might be the reasons for deforestation seen at higher elevation

zones in both the transition matrices A and B, despite the widespread implementation of community forestry in these ecological belts. Siddiqui, Jamil, and Afsar (2004) from their studies in the Sindh-Pakistan reported environmental consequences of deforestation at similar high elevations that not only led to the degradation and erosion of soil, but also caused sedimentation impacts in water bodies at lower elevations downstream. They concluded that each year because of the intertwining interactions of anthropogenic and natural factors, many forested lands degrade, which in turn reduce agricultural production leading to further agricultural expansion into forest areas as the cycle repeats itself. This finding clearly meshes with our model outcomes, where variables such as, people depending upon land, livestock, and poultry clearly explain the process of deforestation in the high elevation zones and also contribute to deforestation at the lower elevations.

**6.2 Conclusion:**

In this paper, we first identified the spatial driving forces (SDFs) of deforestation from a theoretical perspective by reviewing deforestation literature and then relating them to the specific cultural context and geographic particularity of the Central Development Region (CDR) of Nepal. Then we conducted a visual spatial analysis by combining various spatial layers derived from a set of spatio-temporal remote sensing imagery (Figures 3 & 5). In this process, we projected and re-projected maps to compare the alignments of some of the GIS files available from the Department of Survey of Nepal Government, which were projected to UTM 44.5 N. These projections and re-projections

into UTM Zone 45 N, modified UTM Zone 44.5 N, latitude and longitude, and vice-versa using appropriate parameters made it possible to compare and integrate land use and cover information from different records (Figures 5 and 7).

We observed that large areas of forests have been degraded and fragmented in CDR due to the growth of population and its re-settlement and to infrastructure development. Among the forests of this region, maximum deforestation has occurred in tropical and sub-tropical belts (30-1,199 m) close to the roads and human settlements, with decreasing deforestation in the temperate region (1,200 – 2,399 m) and alpine and sub-alpine sub-regions (2,400-4,999 m) with low population density and infrastructure. With the region's economy based on subsistence farming and with the forests being the main source of energy (firewood), fodder (animal feed), and constructional materials (timber) for the majority of the people, deforestation adjacent to human settlements has become a ubiquitous common process, occurring everywhere as time passes. Almost all economic levels of people use the local forests as essential sources for cooking fuel, timber for constructional purposes, and for animal grazing (fodder collection and free-range activities being common). Those with few other sources of income also harvest lumber to sell. Subsistence farmers have strong motivation to clear forests for farming, especially in the lower elevation zones.

Our model outcomes reveal a strong relationship between the farmland and deforestation at all elevation levels. Nepal's overall economy is based on farming and there is a strong linkage between farm and forestry. People with farm and livestock depend upon forest products for their livelihood. Such farmers often take advantages of political unrest to use forest resources, and especially in the last decade of 1990-2000 the level of unrest caused by the Maoist-led "peoples'

war" has been excessive. This finding is similar to Etter *et. al.*'s (2006) in their studies of Colombian regional agricultural patterns and relationships with political unrest. Our models also reveal massive deforestation during the 1990-2000 in the tropical and sub-tropical belts (Model Ib, Figures 7 and 9) when (and where) the "people's war" was at its most vicious.

The above account reveals that the process of deforestation in CDR of Nepal is diverse in space and time with rapid deforestation still occurring in areas outside the national parks and wildlife reserves. A review of literature and our models' hypotheses suggested that infrastructure networks are likely to have important impacts on deforestation activities (Figures 6,7 and 9), and Models'(I and II) outcomes showing the significance of "distance to forests from road" on deforestation justify this assumed association (Tables 1.2).

Our overall findings are similar to the findings of the Food and Agricultural Organizations of the United Nations, which states that human activities are responsible for permanent losses of forest cover, or at least for leaving long-lasting legacies to alter forest structure and compositions, even under conditions of subsequent afforestation (FAO, 2007). We identified many proximate causes and driving forces of deforestation that were far exceeding the rates of afforestation (Table 1.1; Figure 9).

In summary, we identified the spatial driving forces (SDFs) of deforestation in CDR for 1975-1990 and 1990-2000. Our rigorous VDC and municipality levels identification of landuse and land cover dynamics by elevation classes coupled with demographic and socioeconomic information suggest that deforestation in CDR has been and still is related to multiple factors; some of which differ across ecological zones and elevations. We used highly detailed spatially explicit satellite data on forest delineation, undertook rigorous data collection through overlay processes and estimated regression models by integrating sociodemographic, socioeconomic, and

biophysical data to assess the relative strengths of which potential determinants turn out to be important region-wide, or in one or more zones. The procedures used here have produced significant, policy-relevant results, and we argue that our analytical approach would be applicable in other cases of South Asian deforestation, where similar sociodemographic, socioeconomic, biophysical, and governance conditions prevail (though civil unrest and a "peoples' war" should not be a pre-requisite, obviously). Further, we argue that our analysis is quantitatively rigorous because we incorporated the most recent available information comprised of anthropogenic and biophysical variables, whose effects have not been evaluated at this regional scale, nor have they utilized such small administrative units as VDCs as the operating unit of observation. Also, to add further to the examination of deforestation in the three regions of the CDR – the mountains, hills and Tarai plains - we have used specific elevation levels as operational surrogates for ecological zones of interest, so that the resultant ecological and biophysical differentiation within the VDC units can be better represented and analyzed.

**ACKNOWLEDGEMENTS**

This research is supported by an Indiana Space Grant, by the Ford Foundation, and a University Research Grant from the Office of Sponsored Programs and the College of Arts, Humanities, and Social Sciences of the University of Central Missouri (19-SU003). This research would not have been completed without the data access to NASA Land Processes Distributed Active Archive Center (LP DAAC) and data support from Principal Scientist Dr. Chandra Giri of USGS. Special Thanks to Prof. Nanda R. Shrestha for his insightful guidance to this research.

**7. References:**

Armenteras, D., G. Rudas, N. Rodriguez, S. Sua, and M. Romero (2005). Patterns and causes of deforestation in the Amazon. *Ecological Indicators*, 6: 353-368.

Aspinall, R. (2004). Modelling land use change with generalized linear models—a multi-model analysis of change between 1960 and 2000 in Gallatin Valley, Montana. *Journal of Environmental Management*, 72: 91-103.

Bajracharya, D. (1983). Deforestation in the food/fuel context: Historical and political perspectives from Nepal. *Mountain Research and Development*. 3: 227-240.

Bhattarai, Keshav and Dennis Conway (2008)**.** Evaluating Land Use Dynamics and Forest Cover Change in Nepal's Bara District (1973-2003). *Human Ecology: An Interdisciplinary Journal*. Volume 36, Number 1 / February, 2008

Bhattarai, K. (2001). *Household landownership and the use of forests in the Bara district of Central Tarai Region of Nepal*. Unpublished Ph. D. Dissertation, Indiana University, Bloomington, Indiana.

Bhattarai, K., Conway, D., and Shrestha, N. R. (2002). The vacillating evolution of forestry policy in Nepal: Historically manipulated, internally mismanaged. *International Development Planning Review,* 24(3), pp. 315-38.

CBS (2007) Central Bureau of Statistics, Government of Nepal, Katmandu.

Chaudhary, R. P. (2000). Forest conservation and environmental management in Nepal: A review, *Biodiversity and Conservation* 9: 1235-1260

Chowdhury, R. R. (2006). Driving forces of tropical deforestation: The role of remote sensing and spatial models. *Singapore Journal of Tropical Geography*, 27: 82-101

Chomitz, K. M. and T. S. Thomas (2003). Determinants of land use in Amazonia: A fine-scale spatial analysis. *American Journal of Agricultural Economics*, 85: 1016.

Deininger, K. and B. Minten (2002). Determinants of deforestation and the economics of protection: an application to Mexico. *American Journal of Agricultural Economics*, 84(4): 943-960.

Dull, Robert A. (2007). Evidence for Forest Clearance, Agriculture, and Human-Induced Erosion in Precolumbian El Salvador. *Annals of the Association of American Geographers*, 97(1), 2007, pp. 127–141

Earth Resources Observation and Science (EROS) http://edc.usgs.gov/.

Etter, A., C. McAlpine, K. Wilson, S. Phinn, and H. Possingham (2006). Regional patterns of agricultural land use and deforestation in Colombia. *Agriculture, Ecosystems and Environment*, 114: 369-386.

FAO (2001). *Global Forest Resources Assessment 2000 Main Report*. Food and Agricultural Organization, Rome.

Ferreira, N. C., L. G. Ferreira, A. R. Huete, and M. E. Ferreira (2006). An operational deforestation mapping system using MODIS data and spatial context analysis. *International Journal of Remote Sensing*, Vol. 28 (1): 47-62.

Geist, H. J. and E. F. Lambin (2002). Proximate causes and underlying driving forces of tropical deforestation. *Bioscience*, 52: 143-150.

Geoghegan, J., V. S. Cortina, P. Kelpies (2001). Modeling tropical deforestation in the southern Yucatan peninsular region: Comparing survey and satellite data. *Agricultural Ecosystems and Environment*, 85: 25-46.

Gilmour, D. A., and R. J. Fisher (1991) *Villagers, Forests and Foresters: A Philosophy, Process and Practice of Community Forestry in Nepal.* Sahayogi Press, Tripureswor, Kathmandu, Nepal.

Hardin, G. (1968). The Tragedy of the Commons, *Science*. December, pp. 1243.

Irwin, E. G. and J. Geoghegan (2001). Theory, data, methods: developing spatially explicit economic models of land use change. *Agriculture, Ecosystems and Environment*, 85 (1-3): 7-23.

Ives, J.D. and B. Messerli (1989*) The Himalayan Dilemma: Reconciling Development and Conservation*. The United Nation University, Routeledge, London and New York.

Kaimowitz, D. and A. Angelsen (1998). *Economic Models of Tropical Deforestation: A Review*. CIFOR, Bogor.

Laney, R. M. (2004). A process-led approach to modelling land change in agricultural landscapes: A case study from Madagascar. *Agriculturae, Ecosystems, and Environment*, 101: 135-153.

Lillesand, T. M., Keifer, R. W., and Chipman, J. W. (2008). *Remote Sensing and Image Interpretation*. Sixth edition, Wiley.

Mertens, B. and E. F. Lambin (2000). Land cover change trajectories in southern Cameroon. Annals of Association of

Monserud, R.A. and Leemans, R. (1992). Comparing global vegetation maps with the Kappa statistics. *Ecological Modelling* 62: 275-293.

Muller-Boker, Ulrike (1999). *The Chitwan Tharus in Southern Nepal: An Ethnological Approach*. Frnaz Stener Verlag Stuttgart.

Munroe, D. K., J. Southworth, and C. tucker (2004). Modelling spatially and temporally complex land cover change: The case of western Honduras. *The Professional Geographer*, 56 (4): 544-559.

Nelson, G. C. and D. Hellerstein (1995). Do roads cause deforestation? using satellite image in econometric analysis of land use. *American Journal of Agricultural Economics*, 79.

Nelson, G. C. V. Harris, and S. W. Stone (2001). Deforestation, land use, and property rights: Empirical evidence from Darien, Panama. *Land Economics*, 77: 187-205.

Nepal, M., A. Bohara, and R. P. Barrens (2007). The impacts of social networks and household forest conservation efforts in rural Nepal. Land Economics, 83(2): 66-83.

Nepstad, D. C., V. Varoassimo, A. Alencar, C. Nobre, E. Lima, P. Lefebvre, P. Schlesinger, C. Potterk, P. Moutinho, E. Mendoza, M. Cochrane, and V. Brooks (1999). Large-scale improvement of Amazonian forests by logging and fire. *Nature*, 398: 505-508.

Pfaff, A, J.Robalino, R. Walker, S. Aldrich, M. Caldas, E. Reis, S. Perz, C. Bohrer, E. Arima, W. Laurance, and K. Kirby (2007). Road investments, spatial spillover, and deforestation in the Brazillian Amazon. *Journal of Regional Science*, Vol. 47(1): 109-123.

Pfaff, A. (1999). What drives deforestation in the Brazilian Amazon? *Journal of Environmental Economics and Management*, 37: 26-43.

Quincey, D. J., A. Luckman, R. Hussel, R. Davies, P. L. Sankhayan, and M. K. Balla (2006). Fine-resolution remote-sensing ad modelling of Himalayan catchment sustainability. *Remote Sensing and Environment*, 107: 430-439.

Rindfuss, r. J. fox, and S. J. Walsh (2003). *People and the Environment: Approaches for Linking Household and Community Survey to Remote Sensing and GIS*. Kluwer, Boston.

Rindfuss, R. R., B. Entwisle, S. J. Walsh, C. F. Mena, C. M. Erlien, and Cl. L. Gray (2007). Frontier land use changes: Synthesis, challenges, and next steps. *Annals of the Association of American Geographers*, 97(4): 739-754.

Rudel, T. K. (1989). Population development, and tropical deforestation: A cross national study. *Rural Sociology*, 54: 327-338.

Ruttan, V. W. and Y. Hayami (1984). Towards a theory of induced institutional innovation. *Journal of Development Studies*, 20: 203-223.

Sader, S. A. (1995). Spatial characteristics of forest clearing and vegetation re-growth as detected by Landsat Thematic Mapper Imagery. *Photogrammetric Engineering and Remote Sensing*, 61 (9)**,** pp. 1145-11451.

Semwall, D. P., P. Pardha Saradhi1, B. P. Nautiyal and A. B. Bhatt (2007). Current status, distribution and conservation of rare and endangered medicinal plants of Kedarnath Wildlife Sanctuary, Central Himalayas, India. *Current Science* 1734, Vol. 92 (12), 25 June.

Sen, K. K., K. S. Rao, and K. G. Saxena (1997). Soil erosion due to settled upland farming in Himalaya: A case study in Pranmati watershed. *International Journal of Sustainable Development and World Ecology*, 4: 65-74.

Shrestha, N. R., D. Conway, and K. Bhattarai (1999). Population Pressure and Land Resources in Nepal: A Revisit, Twenty Years Later, *The Journal of Developing Areas*, 33 (Winter): 245-268.

Skole, D. and C. Tucker (1993). Tropical deforestation and habitat fragmentation in the Amazon: Satellite data from 1978 to 1988. *Science*, 260: 1905-1910.

Siddiqui, M. N. Z. Jamil and J. Afsar (2004). Monitoring changes in riverine forests of South-Pakistan using remote sensing and GIS techniques. *Advance in Space Research*, 33: 333-337.

Soares-Filho, B., D. Nepstad, L. Curran, G. Carqueira, R. Garcia, C. A. Ramos, E. Voll, A. Mcdonald, P. Lefebvre, and P. Schlessinger (2006). Modeling conservation in the Amazon basin. *Nature*, 440: 520-523.

The Land Processes Distributed Active Archive Center http://edcdaac.usgs.gov/dataproducts.asp

Tiwari, P. C. (2000). Land-use changes in Himalaya and their impact on the plains ecosystem: Need for sustainable land use. *Land Use Policy*, 17: 101-111.

Turner, M. G., D. N. Wear, and R. O. Flamm (1996). Land ownership and land cover change in the southern Appalachian highlands and the Olympic peninsula. *Ecological Applications*, 6(4): 1150-1172.

University of Maryland: ftp://ftp.glcf.umiacs.umd.edu/glcf/Landsat/WRS2/

Varughese, G. (2000) *Villagers, Bureaucrats, and Forests in Nepal: Designing Governance for a Complex Resource*. Unpublished Dissertation Submitted to Indiana University to the School of Public and Environmental Affairs and the Department of Political Science, Indiana University, Bloomington, Indiana.

Vasquez-Leon, M. and D. Liverman (2004). The political ecology of land use change: Affluent ranchers and destitute farmers in the Mexican municipio of Alamos. *Human Organization*, 63(1): 21-23.

Verma, A. (2002). Data sources and measurement technologies for modeling. In Clarke, K. C., B. O. Parks, and M. P. Crane (eds) *Geographic Information Systems and*

*Environmental Modeling*. Prentice Hall, Upper Saddle River, New Jersey 07458. p67-99.

Walker, R. T. (2004). Theorizing land-cover and land-use change: The case of tropical deforestation. *International Regional Science Review*, 27(3): 247-270.

Walker, R. T. and W. D. Solecki (2004). Theorizing land-cover and land-use change: The case of the Florida Everglades and its degradation. *Annals of the Association of American Geographers*, 94(2): 311-318.

Whitemore, T. C. (1997). Tropical forest disturbance, disappearance, and species loss. In: Laurance, W. F., R. O. Bierrengaard Jr. (eds). *Tropical Forest Remnants: Ecology, Management and Conservation of Fragmented Communities*: 3-12.

Table 1.1
MODEL I: Tropical and Subtropical Sub-regions
Number of observations used: 1085

| **MODEL IA: DEFORESTATION 1975-1990 (30-1,199 M)** | | | | | **MODEL IB: DEFORESTATION 1990-2000 (30-1,199 M)** | | | | |
|---|---|---|---|---|---|---|---|---|---|
| **Source** | **DF** | **Sum of Square** | **Mean Square** | **F (Pr>F)** | **Source** | **DF** | **Sum of Square** | **Mean Square** | **F (Pr>F)** |
| Model | 11 | 1.526E16 | 1.387E15 | 195.55 <0.0001 | Model | 11 | 4.689E16 | 4.263E15 | 1705.19 <0.0001 |
| Error | 1073 | 7.613E15 | 7.095E12 | | Error | 1073 | 2.683E15 | 2.499E12 | |
| Corrected Total | 1084 | 2.288E16 | | | Corrected Total | 1084 | 4.95E16 | | |
| Root MSE | | 2663705 | $R^2$ | 0.6672 | Root MSE | | 1581060 | $R^2$ | 0.9459 |
| Dependent Mean | | 4243803 | Adj $R^2$ | 0.6638 | Dependent Mean | | 7005149 | Adj $R^2$ | 0.9453 |
| Coefficient Variance | | 62.7669 | | | Coefficient Variance | | 22.579 | | |
| **PARAMETER ESTIMATES: 1975-1990** | | | | | **PARAMETER ESTIMATES: 1990-2000** | | | | |
| **Variables** | **Parameter Estimate** | **Std. Error** | **t-value** | **Pr> \|t\|** | **Variables** | **Parameter Estimate** | **Std. Error** | **t-value** | **Pr> \|t\|** |
| Intercept | 730452 | 152034 | 4.80 | <.0001 | Intercept | 87051 | 94752 | 0.92 | 0.3584 |
| Immigrants from other VDCs | 1350.85 | 105.85 | 12.76 | <.0001 | Population depending on farming | 170.89 | 65.39 | 2.61 | 0.0091 |
| Immigrants other municipalities | -11418 | 985.71 | -11.6 | <.0001 | Population depending on farm and livestock | 2.48 | 1.56 | 2.14 | 0.0322 |
| Population (trade) | -463.87 | 181.47 | -2.56 | <.0107 | Pop. on farm, livestock, & poultry | 176.05 | 40.99 | 4.30 | <.0001 |
| Population (trans) | 3185.98 | 1119.7 | 2.85 | <.0045 | Total population | 613.76 | 156.45 | 3.92 | <.0001 |
| Male (20-24 yrs) | -16393 | 2147.2 | -7.63 | <.0001 | Immigrants same VDCs | -651.24 | 171.62 | -3.79 | 0.0002 |
| Male (25-29 yrs) | 15343 | 2188.6 | 7.01 | <.0001 | Immigrants other VDCs | -535.30 | 156.43 | -3.42 | 0.0006 |
| Female (30-34yrs) | 8610.85 | 1343.6 | 4.94 | <.0001 | Female (15-19 yrs) | 686.36 | 686.36 | -2.55 | 0.0110 |
| Farmland 1975 | -0.0822 | 0.035 | -2.34 | <.0196 | Farmland 1990 | -0.2525 | 0.0179 | -14.1 | <.0001 |
| Farmland 1990 | 0.36865 | 0.0186 | 19.81 | <.0001 | Farmland 2000 | 0.9523 | 0.0131 | 72.55 | <.0001 |
| Highway 1975 | -260.47 | 71.65 | -3.64 | <.0003 | Distance from road | 1.9438 | 0.259 | 7.50 | <.0001 |
| Elevation | 0.041 | 0.0022 | 18.94 | <.0001 | All elevation | -0.00315 | 0.0017 | -1.84 | 0.0663 |
| Durbin-Watson D = 1.782<br>1st Order autocorrelation = 0.099 | | | | | Durbin-Watson D = 1.739<br>1st Order autocorrelation = 0.100 | | | | |

Table 1.2
Model II: Temperate sub-region, Number of observations: 609

| **MODEL IIA: DEFORESTATION 1975-1990 (1,200–2,399 M)** | | | | | **MODEL IIB: DEFORESTATION 1990-2000 (1,200 – 2,399 M)** | | | | |
|---|---|---|---|---|---|---|---|---|---|
| **Source** | **DF** | **Sum of Square** | **Mean Square** | **F (Pr>F)** | **Source** | **DF** | **Sum of Square** | **Mean Square** | **F (Pr>F)** |
| Model | 3 | 8.243E15 | 2.748E15 | 269.39 <0.0001 | Model | 5 | 3.5925E16 | 7.185E15 | 2060.55<.0001 |
| Error | 605 | 6.171E15 | 1.028E12 | | Error | 603 | 2.1027E15 | 3.487E12 | |
| Corrected Total | 608 | 1.442E16 | | | Corrected Total | 608 | 3.8028E16 | | |
| Root MSE | | 3193702 | $R^2$ | 0.5719 | Root MSE | | 1867351 | $R^2$ | 0.9447 |
| Dependent Mean | | 3625242 | Adj $R^2$ | 0.5698 | Dependent Mean | | 6605909 | Adj $R^2$ | 0.9442 |
| Coefficient Variance | | 88.0962 | | | Coefficient Variance | | 59.6759 | | |

| **PARAMETER ESTIMATES: 1975-1990 (1,200 – 2,399 M)** | | | | | **PARAMETER ESTIMATES: 1990-2000 (1,200 – 2,399 M)** | | | | |
|---|---|---|---|---|---|---|---|---|---|
| **Variables** | **Parameter Estimate** | **Std. Error** | **t-value** | **Pr>\|t\|** | **Variables** | **Parameter Estimate** | **Std. Error** | **t-value** | **Pr>\|t\|** |
| Intercept | -132277 | 188755 | -0.70 | 0.4837 | Intercept | -25395 | 111845 | -0.23 | 0.8250 |
| Population on livestock, poultry | 11404 | 1686.5 | 6.76 | <.0001 | Population on livestock, poultry | 2926.51 | 1373.5 | 2.13 | 0.0335 |
| Farmland 1975 | 0.12728 | 0.0418 | 3.04 | <.0025 | Immigrants same VDC | -28.24083 | 6.642 | -4.25 | <.0001 |
| Farmland 1990 | 0.4068 | 0.0216 | 18.84 | <.0001 | Distance from road | 1.759 | 0.4376 | 4.02 | <.0001 |
| | | | | | Farmland 1990 | -0.19256 | 0.0226 | -8.51 | <.0001 |
| | | | | | Farmland 2000 | 0.89755 | 0.0196 | 45.70 | <.0001 |
| Durbin-Watson D = 1.745<br>1st Order autocorrelation = 0.111 | | | | | Durbin-Watson D = 1.583<br>1st Order autocorrelation = 0.170 | | | | |

Table 1.2
Model III: Sub-alpine and Alpine sub-region
Number of observations: 221

| **MODEL IIIA: DEFORESTATION 1975-1990 (2,400 – 4,999 M)** | | | | | **MODEL IIIB: DEFORESTATION 1990-2000 (2,400 – 4,999 M)** | | | | |
|---|---|---|---|---|---|---|---|---|---|
| **Source** | **DF** | **Sum of Square** | **Mean Square** | **F (Pr>F)** | **Source** | **DF** | **Sum of Square** | **Mean Square** | **F (Pr>F)** |
| Model | 2 | 4.844E15 | 2.422E15 | 168.63 <0.0001 | Model | 2 | 2.8171E16 | 1.408E15 | 3119.42 <0.0001 |
| Error | 218 | 3.131E15 | 1.436E12 | | Error | 218 | 9.8434E14 | 4.545E12 | |
| Corrected Total | 220 | 7.975E16 | | | Corrected Total | 220 | 2.9154E16 | | |
| Root MSE | | 37898 | $R^2$ | 0.6074 | Root MSE | | 2124930 | $R^2$ | 0.9662 |
| Dependent Mean | | 4335526 | Adj $R^2$ | 0.6038 | Dependent Mean | | 9015751 | Adj $R^2$ | 0.9659 |
| Coefficient Variance | | 87.4131 | | | Coefficient Variance | | 23.5691 | | |

| **PARAMETER ESTIMATES: 1975-1990 (2,400 – 4,999 M)** | | | | | **PARAMETER ESTIMATES: 1990-2000 (2,400 – 4,999 M)** | | | | |
|---|---|---|---|---|---|---|---|---|---|
| **Variables** | **Parameter Estimate** | **Std. Error** | **t-value** | **Pr> \|t\|** | **Variables** | **Parameter Estimate** | **Std. Error** | **t-value** | **Pr> \|t\|** |
| Intercept | 2193779 | 295794 | 7.42 | <.0001 | Intercept | 503472 | 179261 | 2.81 | 0.0054 |
| River meandering 1990 | -0.60003 | 0.2611 | -2.30 | 0.0225 | River meandering 2000 | 0.63672 | 0.1124 | 5.67 | <.0001 |
| Elevation | 0.13556 | 0.0087 | 15.58 | <.0001 | Farmland 2000 | 0.74875 | 0.0135 | 55.51 | <.0001 |
| Durbin-Watson D = 1.572<br>1st Order autocorrelation = 0.213 | | | | | Durbin-Watson D = 1.880<br>1st Order autocorrelation = 0.053 | | | | |